

# 3D augmented reality applied to the treatment of neuropathic pain

B Penelle<sup>1</sup>, D Mouraux<sup>2</sup>, E Brassinne<sup>2</sup>, T Tuna<sup>3</sup>, A Nonclercq<sup>4</sup>, N Warzée<sup>1</sup>

<sup>1</sup>LISA Laboratory, <sup>4</sup>LIST Laboratory, Université Libre de Bruxelles,  
50 av. F-D Roosevelt, 1000 Brussels, BELGIUM

<sup>2</sup>Centre de réadaptation de l'appareil locomoteur,

<sup>3</sup>Department of Anaesthesiology, Pain Clinic, Erasme Hospital,  
Route de Lennik 808, 1070 Brussels, BELGIUM

*benoit.penelle@ulb.ac.be, dominique.mouraux@ulb.ac.be*

*<sup>1</sup>lisa.ulb.ac.be, <sup>2</sup>www.erasme.ulb.ac.be*

## ABSTRACT

Neuropathic pain is characterized by a permanent or recurrent background pain including stinging, tingling, allodynia, burning, shock or stabbing sensations. It significantly alters the patient quality of life. Such painful conditions are observed in the case of phantom limb pain (PLP) and complex regional pain syndrome (CRPS), and are difficult to treat effectively. Recent studies show the crucial role of the central nervous system in these pathologies and suggest a link to the plasticity of the latter. Mirror visual feedback (MVF) is often used in case of amputation, CRPS or stroke to restore normal cortical organization and to lower pain intensity. We have conceived an augmented reality (AR) system that applies the principle of MVF without requiring the use of a physical mirror. The system strengthens the patient's immersion and concentration by using realistic, natural looking 3D images that are acquired, processed and displayed in 3D, in real time. Our system is based on standard inexpensive hardware and is easy to install and to use. This makes it perfectly suitable for use in a therapist's practice or at home. The preliminary results of clinical tests show that the system can significantly reduce the pain, after only a few training sessions.

## 1. INTRODUCTION

Neuropathic pain is defined by the International Association for the Study of Pain (IASP) as "pain initiated or caused by a primary lesion or dysfunction in the nervous system" (IASP, 1994). Many patients with neuropathic pain present persistent or paroxysmal pain. This stimulus-independent pain can be lancinating, burning and also characterized by symptoms like stinging, tingling, allodynia, burning, shock or stabbing sensations... In this context phantom limb pain (PLP) and complex regional pain syndrome (CRPS) are considered as neuropathic pain, and most recommendations are recommendations for neuropathic pain syndromes.

Phantom sensations are the non-painful or painful sensations experienced in the body part that no longer exists. The prevalence of PLP is more common among upper limb amputees than lower limb amputees (Subedi and Grossberg, 2011). The most commonly description of pain is tingling, throbbing, piercing and pins or needles sensations.

CRPS is a weakening, painful condition in a limb, associated with sensory, motor, autonomic, skin and bone abnormalities. It appears commonly after injury to that limb. Limb signs such as sweating, swelling and color changes usually reduce with time. Unfortunately pain persists. The aetiology of CRPS is unknown. Characteristically, there is interplay between peripheral and central pathophysiology.

Cortical reorganization is one reason evoked for the cause of PLP and CRPS. During reorganization, the cortical areas representing the amputated extremity are taken over by the neighboring representational zones in both primary somatosensory and the motor cortex. The extent of cortical reorganization has been found to be directly related to the degree of pain and the size of the deafferented region. In CRPS, several studies have indicated that cortical reorganization plays a role in the persistence of the symptoms.

Recent advances in neuroscience and cognitive science have opened up new possibilities to treat this kind of pathology. A relatively new way to decrease pain and to improve function for the patients with upper limb

disabilities is to use the visual feedback provided by mirror therapy. Mirror therapy or mirror visual feedback (MVF) was first reported by Ramachandran and Rogers-Ramachandran (1996) and is suggested to help PLP patients by resolving the visual proprioceptive dissociation in the brain.

The principle of MVF (Ramachandran and Altschuler, 2009) is simple: using a mirror, the patient observes virtual movements of his affected limb as a mirror reflection of the movements of the opposite healthy limb. Working this way allows one to restore consistency between the motor intention and the visual feedback, which causes cortical reorganization, resulting in a persistent decrease in pain.

Given the positive effect of visual feedback through a mirror in case of phantom pain, and the fact that it gives the illusion that the amputated arm is “alive” again, mirror therapy usage has been extended to other pathologies, like CRPS and stroke with variable success.

In this paper, we present a prototype system that combines 3D Virtual Reality (VR) technologies and the principles of MVF, and how we apply it to the treatment of neuropathic pain.

The usage of VR for the treatment of pain is not recent. Moseley (2007) combined a mirror for the upper part of the body and a projector for the lower part in order to simulate a virtual walking for paraplegic patients. He observed effective reduction of the neuropathic pain endured by the patients. In pilot studies from Murray et al. (2006) and Sato et al. (2010), VR is applied to MVF for treating CRPS or PLP. Their respective setups track the motion of the hand using a data glove and movements of the arm or leg using sensors attached to the limbs of the patients. The problem with this approach is that it requires the patient to be equipped with a quite complex tracking system, making the whole system cumbersome and difficult to use at home. Also, the reconstructed image shown to the patient is a pure virtual arm that hardly looks like his real arm.

## 2. MATERIAL AND METHODS

The main objective we had in mind, when we designed our system, was to increase as much as possible the immersion of the patient. By immersion, we mean the illusion he has that what he sees is the reality. To achieve this, we decided not to work with an approximate representation of the patient in the form of an avatar, but with real 3D images of the patient shown on a 3D display. In that sense, our approach could be parented to an augmented reality (AR) system, according to the definition given by Azuma et al. (2001).

### 2.1 Description of the setup

The patient wears 3D glasses and looks at himself on a 3D screen. A 3D camera captures his movements in real-time and the system augments this 3D reality in two ways : (1) by performing some specific image processing, like lateral flipping or applying a virtual mirror as we will explain later, and (2) by adding to the scene some virtual objects of different shapes and sizes with which the patient may interact.

The 3D camera is the Kinect™ from Microsoft. It produces depth and color images that are synchronized and calibrated, at a rather good resolution (640x480 pixels) and with a good frame rate (30 frame per second), all of that for a rather low cost. For the display, we use the 3D Vision Kit™ from nVidia which offers active stereovision, and a 120 Hz display screen.

### 2.2 Construction of the 3D Images

To construct the 3D images, we use the depth image that is delivered by the Kinect and we transform it to a set of points (also called vertices) in the 3D space, or point cloud in the literature, by using the calibration parameters of the camera. After that, the system meshes these vertices together based on their relative positions in the depth image (Figure 1, top left) and applies them a texture by using the color image coming from the Kinect (Figure 1, top right).

A straightforward method to construct a mesh from a point cloud consists in finding the nearest neighbors for each vertex and connecting them to the vertex with triangles. In a general case, the search for the nearest neighbors is very costly in computation time, and even if there exists algorithms optimized for this task, the computation time is not compatible with our requirement of real-time display. Fortunately, in the current case we can simplify the problem since we have at our disposal the depth image coming from the camera. This image is organized in pixels along two dimensions, each pixel corresponding to a vertex in the point cloud. We will use this 2D pixel organization to pre-determine the neighborhood relationships between the vertices of our point cloud. Figure 2 illustrates how neighbor vertices are connected together based on the 2D organization of their corresponding pixels. This technique works well for triangles that connect vertices belonging to the same surface and that are close to each other in terms of Euclidean distance. But some pixels

that are direct neighbors on the depth image may in reality be located in 3D space at very different depth values, producing distorted (elongated) triangles in the mesh (see red triangles on Figure 1, bottom left). This is typically the case for pixels that correspond to the edge of an object. After identification and removal of these bad triangles we obtain a nice and clean 3D mesh (Figure 1, bottom right).

This whole process has to be repeated for each depth image that comes from the camera, 30 times per second. In reality, the computation has to be even faster than that because in order to display a 3D image on the screen with stereovision, we have to generate two different views of it, one for each eye. To be able to sustain such a frame rate, we let this process run on the highly parallel architecture of the graphics card. We pre-load a static mesh organization that matches the organization of the pixels in the 2D image. When the graphics pipeline is ready to render a triangle of the mesh, it calls a specific geometry shader. This shader determines whether the current triangle may be rendered based on two simple criteria: (1) it requires that each vertex of the triangle has a depth value contained in a given range, (2) it also requires that the maximum depth difference between the three vertices of the triangle is smaller than a certain threshold (in our case 3 cm). If these criteria are not met, the geometry shader discards the triangle and it is not rendered. The geometry shader acts thus as a filter on the triangles.

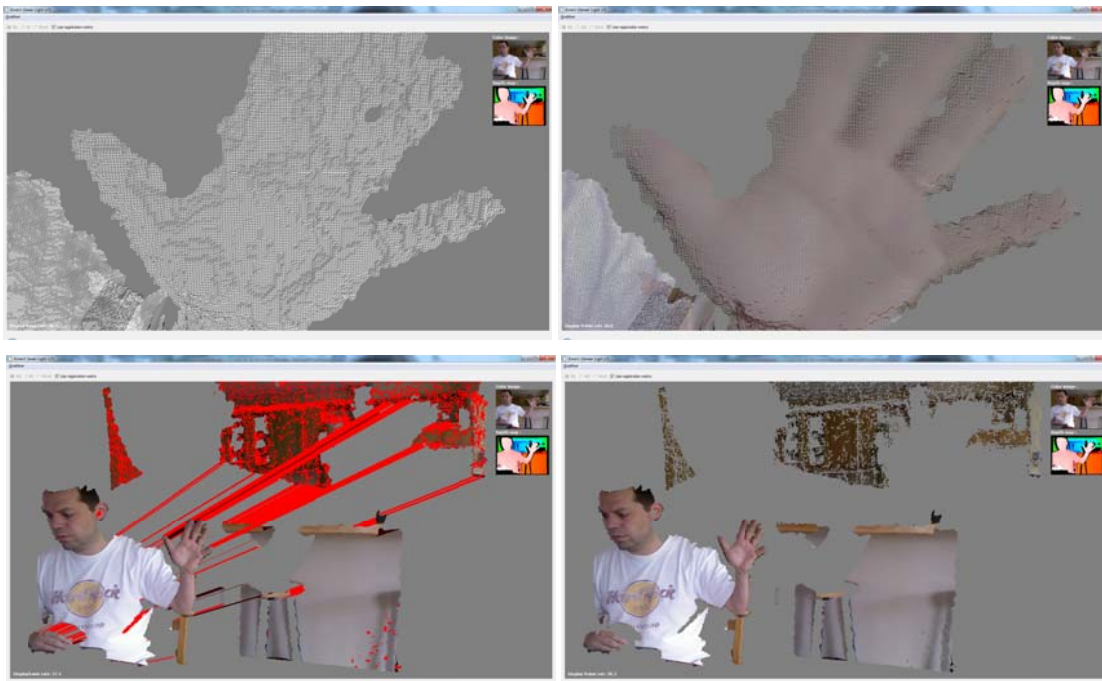


**Figure 1.** Successive steps involved in the construction of the textured 3D mesh starting from the point cloud coming from the Kinect.

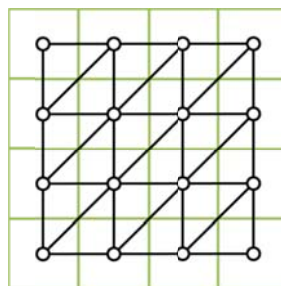


**Figure 2.** The connectivity between the vertices of the mesh is defined based on the 2D organization of the pixels (green boxes) in the depth image. It results in a set of triangles (shown in black).

Since we work with one camera, we can only reconstruct the portion of the volume that is visible with the camera, that is to say the frontal part of the volume of the patient's body. This may give the impression that we lack a part of the image. We are also limited by the resolution of the depth image produced by the Kinect (640x480 pixels). Despite these limitations, the quality of the generated images is quite good and is certainly

sufficient for the use we make of it (Figure 3). Moreover, the fact that the patient watches the images in 3D strengthens the perception of quality and realism.

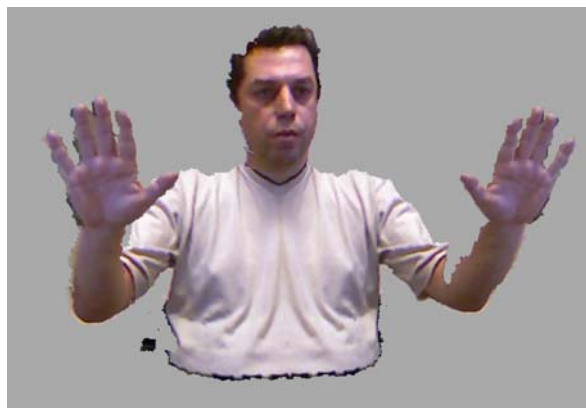


**Figure 3.** Sample frame to illustrate the quality of the generated images.

### 2.3 Application of the mirror effect

By convention, the 3D frame of reference of our system is the one of the camera. The origin is at its focal point and the Z axis corresponds to the focal axis. The X and Y axes correspond respectively to the horizontal and vertical axes of the camera.

The virtual mirror is defined by a plane which is always positioned vertically and perpendicularly to the focal plane of the camera, that is to say parallel to the YZ plane. The only degree of freedom of the mirror is a lateral displacement along the X axis. The system also manages a parameter that determines which side of the mirror is the reflecting one. The application of the mirror is very straightforward: all the triangles of the mesh that are located on the non-reflective side of the mirror are removed and all those that are on the reflective side are duplicated symmetrically with respect to the mirror's plane (see Figure 4).

At this stage, there still remains an issue to tackle: the mirror effect works well for the trunk and the arms showing quite convincing results. But the result on the face is rather disgraceful (see Figure 5). To solve this, we have defined a “safe zone” around the head of the patient where the effect of the mirror is not applied (see Figure 4, middle and right images).

This part of the algorithm is also implemented as a specific geometry shader.

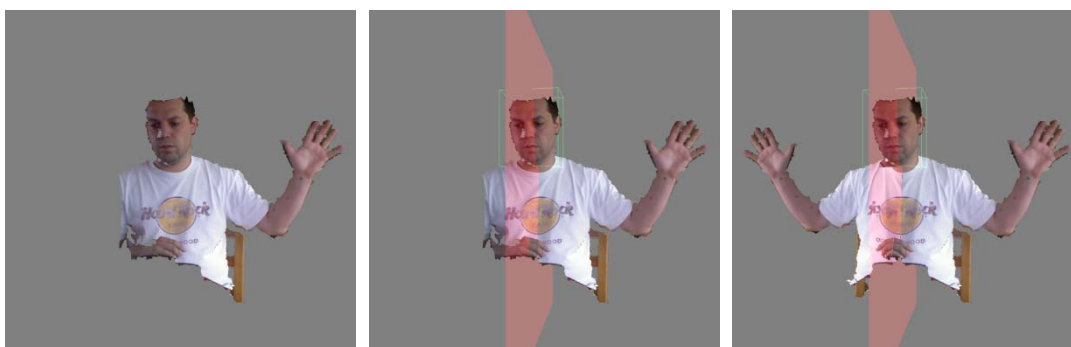


**Figure 4.** Application of a virtual mirror to a 3D image. The left part shows the original image. In the middle part we see the virtual mirror in pink and the safe zone in green. The right part shows how the 3D mesh that is on the right side of the mirror is duplicated symmetrically to the left side, except inside the safe zone.

### 2.4 Automatic positioning of the mirror

Even if the patient sits still in front of the screen and tries to move only his arm, we observe small movements of the other parts of his body like the head or the trunk. The visual side effect of these parasite movements is that the patient seems to go partially in and out of the mirror. To get rid of this, we have implemented a visual tracking of the patient's head position at each frame. We use this position to automatically place the mirror and the safe zone at the center of mass of the head's image.



**Figure 5.** Effect of the “safe zone”: on the left image, the safe zone is not activated, on the right image, it is activated.

To track the head, we proceed as follows: we seek the highest pixel inside a central vertical strip of the depth image. This pixel corresponds approximately to the top of the head. We compute the projection of this pixel in 3D space and we outline a parallelepipedic volume centered on this point in X and Z and placed below it in Y. This volume is dimensioned to be certain to contain any patient's head and possibly the beginning of the shoulders, even if the upper pixel is not perfectly centered with regards to the head. We then calculate the centroid of all the vertices included in this volume, and their minimum and maximum coordinates. The X coordinate of the centroid gives us the X position of the mirror, while the minimum and maximum coordinates define the “safe zone” around the head.

To prevent the noise in depth data to affect the position of the mirror, we perform a smoothing over time by averaging the mirror positions of the last N frames (N typically equals 2 or 3).

The above algorithm is obviously very specific to our configuration, but it has the advantage of being simple to implement and very fast to compute.

### 2.5 Interaction with virtual targets

To help the patient focus his attention on the movements of the virtual arm, the system implements a very simple game which consists in popping up virtual objects of various shapes and sizes in random positions. The patient is requested to touch these targets with the hand or the fingers of his virtual arm, and when the target is hit, it turns red and disappears. Then, another target appears somewhere else in the game area.

The detection of the “collision” between the hand and the virtual target is done by counting, for each frame, the number of vertices that are located inside the bounding box of the target. If this number exceeds a certain threshold, whose value is a parameter of the system, the target is considered as being touched.

### 2.6 Usage scenarios

We have defined two usage scenarios. The first one consists in applying a virtual mirror to the scene, vertically, so that half of the body of the patient is symmetrically duplicated with regards to the plane of the mirror, as illustrated in Figure 4. The patient has the impression that he is moving both the affected and the non-affected arms.

The second scenario simply consists in inverting the 3D image horizontally, letting the patient observe the reflection of his uninjured arm as if it was the injured one (Figure 6). This scenario is technically speaking a lot easier than the first one because we just have to invert the X coordinates of the mesh vertices.

### 2.7 Typical course of a therapy session

A typical therapy session has a duration of about 15 minutes. It is divided in two phases. First the patient performs some simple exercises with the non-affected arm and watches the virtual movements of the affected arm. The exercises typically are flexions and extensions of the hand, radial-ulnar inclinations of the wrist or tip to tip finger movements.

After that, the patient plays a game where he has to touch, with his virtual hand, virtual targets of different sizes and shapes that appear in random positions in a specific subset of the 3D space called the “game zone” (Figure 7). The difficulty of the game is progressively increased by asking him to first touch the target with the palm, then with the fingers, then to grasp it with the whole hand and finally to grasp it with just the fingers.



**Figure 6.** Illustration of the second scenario: the patient moves his right arm, but he sees its reflection on the other side, as if he was moving his left arm.

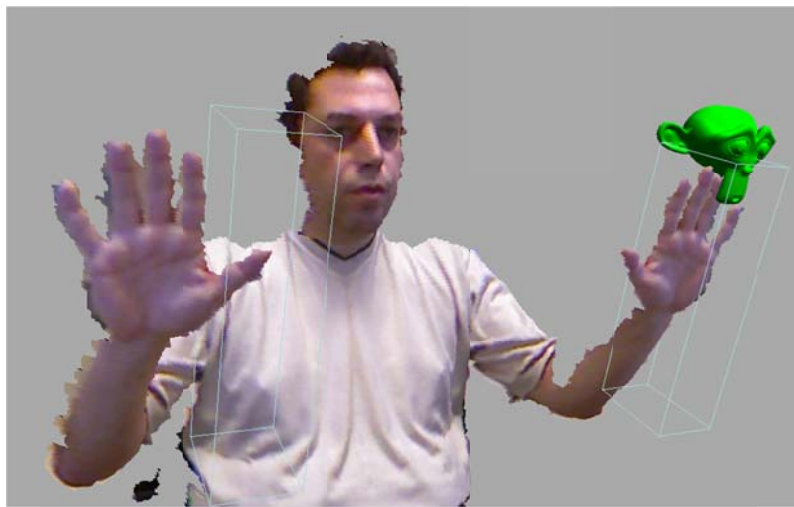


**Figure 7.** The patient plays a game where he has to touch virtual targets with his virtual limb. The two parallelepipeds drawn in cyan wireframe represent the “game zone” where the virtual targets appear.

### 3. RESULTS

All the results presented here have been acquired according to modern ethical standards and have been approved by the ethical committee of the Erasme hospital.

The system has been tested on 8 patients, 7 of them suffering from CRPS and one from PLP after amputation. For each patient, the Table 1 describes the age, the gender, the duration in months of the injury, the initial cause of the pain problem, the affected side and the currently prescribed medication. The medication was not modified or suspended during the treatment.

During the sessions, after five minutes of exercises, the patients have reported one or more of the following effects on the injured side: regional anesthesia, heaviness, tingling, swarming, sleeping effect, sweating.

Figure 8 summarizes the results of the clinical tests. The blue bars represent the pain intensity before starting the therapy session. The violet bars represent the pain intensity at the end of the session. Each patient has performed minimum six sessions and the pain intensity evaluations have been averaged on all the patients. Pain was measured on Visual Analogic Scale (VAS), and we asked the patient to report after how many time the pain reappeared.

From the results obtained for the whole population (Figure 8, left), it may be observed that: (1) the pain intensity decreases on average by 24% between the start and the end of a single session, (2) there is a

persistence effect as the PRE value progressively decreases from one session to the next, and (3) after five sessions, the global pain decrease is of about 32%, on average.

From the results obtained for the sub-population of the four highest responders (Figure 8, right), it may be observed that: (1) the average pain decrease per session is of about 28%, (2) the persistence effect is even stronger, and (3) after five sessions, the average global pain decrease is of about 50%.

We also observe that the pain reduction effect induced during the training persists after the session, during a certain number of hours, and that the duration of this persistence increases with the number of sessions performed (Figure 9). For one patient, the pain totally disappeared after 4 sessions, and for another one after 10 sessions.

**Table 1.** Description of the subjects submitted to clinical tests.

| Subjects | Age | Gender | CRPS or PLP duration | Cause                  | Affected side | Prescribed medications   |
|----------|-----|--------|----------------------|------------------------|---------------|--|
| Case 1   | 48  | ♀      | 6                    | TFCC                   | Left          | Clonazepam   |
| Case 2   | 37  | ♂      | 12                   | Tenolysis              | Right         | Tramadol, amitriptyline, paracetamol                                       |
| Case 3   | 39  | ♂      | 5                    | Suture tendon extensor | Left          | Calcitonine, clonazepam, chlorhydrate tramadol, corticosteroid, pregabalin |
| Case 4   | 75  | ♂      | 4                    | Distal radius fracture | Left          | Duloxetine, paracetamol  |
| Case 5   | 63  | ♀      | 16                   | Wrist instability      | Right         | Nothing  |
| Case 6   | 47  | ♀      | 26                   | Trapezectomy           | Right         | Oxycodone, clonazepam, amitriptyline, duloxetine                           |
| Case 7   | 37  | ♀      | 26                   | Sauve-Kapandji         | Right         | Pregabalin, prazepam, amitriptyline, tramadol                              |
| Case 8   | 36  | ♂      | 60                   | Amputation             | Left          | Oxycodone  |

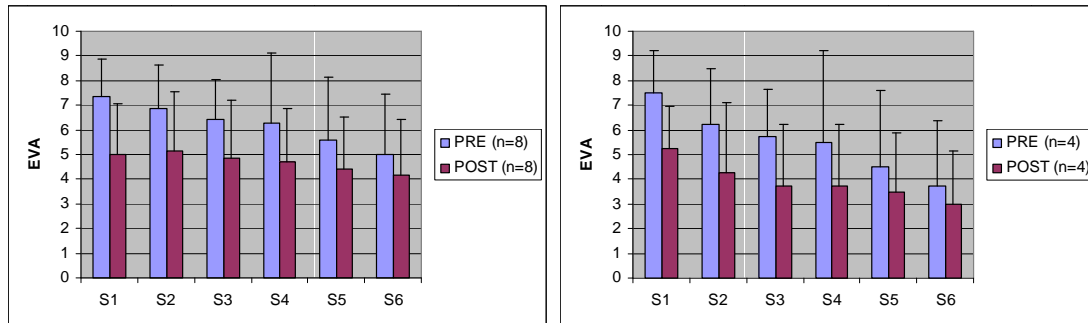


**Figure 8.** PRE and POST pain intensity evaluation for the whole population (left) and for the four highest responders (right).

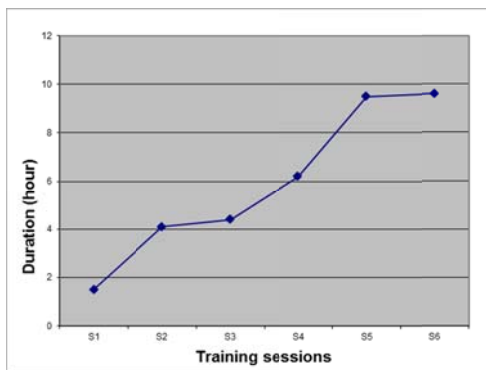


**Figure 9.** Persistence duration of the pain reduction effect as a function of the number of training sessions.

For two subjects, we completed our assessment by measuring a thermal perception and thermal pain threshold with the Neuro Sensory Analyzer (Medoc®). From this measure we have clearly observed a modification in the detection of sensibility (detection was delayed like a hypoesthesia) and also in the perception of pain (almost the same level as of controlateral side). It is too early to draw conclusions from this, but it confirms the symptoms evoked by the patients (anaesthesia, insensibility, decrease of pain ...).

In the future, as proposed by Novak and Katz (2010), in order to confirm our results we will include in our assessments the measures of the physical impairment such as range of motion, strength, and sensibility. Pain assessment using a neuropathic pain scale, like the Mc Gill pain questionnaire to assess both neuropathic and nociceptive pain, will provide information on the intensity of pain. But also self-reported questionnaires such as the Disability Arm Shoulder Hand (DASH), and questionnaires to evaluate for symptoms of depression, pain catastrophizing or fear avoidance will be useful in identifying concomitant psycho-social factors that may affect outcome.

#### 4. CONCLUSIONS

We have developed a system that applies techniques of augmented reality to the principle of the mirror visual feedback. It strengthens the patient immersion and concentration on the movements of the virtual injured arm through the use of 3D image acquisition and display. Since we directly use the 3D and color data from the camera, the generated images are very natural looking, and the patient's illusion that he is moving his injured arm is strengthened. The inclusion of a game where the patient must touch virtual targets positioned randomly in 3D space, allows him to stay focused on the movements of the injured arm throughout the session. It also enables to reduce his anxiety. The system is simple to install and use: the patient must not wear any specific tracking equipment or markers. He simply has to sit in front of the camera and watch the screen with 3D glasses. In addition, through the use of technologies widely available on the market, the system is low cost. All this make our system perfectly suited for use in a therapist's practice or even at home.

The results presented here are preliminary and should be confirmed by a randomized control study on a larger population.

#### 5. REFERENCES

- R Azuma, Y Baillet, R Behringer, S Feiner, S Julier, B MacIntyre (2001), Recent advances in augmented reality. *IEEE Comput. Graph. Appl.*, 21(6), pp. 34–47.
- IASP Task force on taxonomy (1994) Part III : Pain terms - a current list with definitions and notes on usage, In *Classification of chronic pain*, 2nd edition, edited by Merskey H, Bogduk N. Seattle : IASP Press, pp. 209-214.
- G L Moseley (2007), Using visual illusion to reduce at-level neuropathic pain in paraplegia, *Pain*, vol. 130, no. 3, pp. 294–298.
- C D Murray, E Patchick, S Pettifer, T Howard and F Caillette (2006), Investigating the efficacy of a virtual mirror box in treating phantom limb pain in a sample of chronic sufferers, In *Proc. 6<sup>th</sup> Intl Conf. Disability, Virtual Reality & Assoc. Tech.*, Esbjerg, Denmark, pp. 167-174.
- C Novak, J Katz (2010), Neuropathic pain in patients with upper-extremity nerve injury, *Physiotherapy Canada*, vol. 62, no. 3, pp. 190-200.
- V S Ramachandran, D Rogers-Ramachandran (1996), Synaesthesia in phantom limbs induced with mirrors. *Proc. Biol. Sci.*, 263, pp. 377-386.
- V S Ramachandran and E L Altschuler (2009), The use of visual feedback, in particular mirror visual feedback, in restoring brain function, *Brain*, vol. 132, no. 7, pp. 1693–1710.
- K Sato, S Fukumori, T Matsusaki, T Maruo, S Ishikawa, H Nishie, K Takata, H Mizuhara, S Mizobuchi, H Nakatsuka, M Matsumi, A Gofuku, M Yokoyama and K Morita (2010), Nonimmersive Virtual Reality Mirror Visual Feedback Therapy and Its Application for the Treatment of Complex Regional Pain Syndrome: An Open-Label Pilot Study, *Pain Medicine*, vol. 11, no. 4, pp. 622–629.
- B Subedi, G T Grossberg (2011), Phantom limb pain: mechanisms and treatment approaches, *Pain Research and Treatment*, vol. 2011, pp. 1-8.